2014

Positron emission tomographic imaging of Copper 64- and Gallium 68-labeled chelator conjugates of the somatostatin agonist Tyr3-octreotate

Jessie R. Nedrow
University of Pittsburgh

Alexander G. White
University of Pittsburgh

Jalpa Modi
University of Pittsburgh

Kim Nguyen
University of Pittsburgh

Albert J. Chang
University of Pittsburgh

See next page for additional authors

Authors
Jessie R. Nedrow, Alexander G. White, Jalpa Modi, Kim Nguyen, Albert J. Chang, and Carolyn J. Anderson

RESEARCH ARTICLE

Positron Emission Tomographic Imaging of Copper 64– and Gallium 68–Labeled Chelator Conjugates of the Somatostatin Agonist Tyr^3-Octreotate

Jessie R. Nedrow, Alexander G. White, Jalpa Modi, Kim Nguyen, Albert J. Chang, and Carolyn J. Anderson

Abstract

The bifunctional chelator and radiometal have been shown to have a direct effect on the pharmacokinetics of somatostatin receptor (SSTR)-targeted imaging agents. We evaluated three Y3-TATE analogues conjugated to NOTA-based chelators for radiolabeling with ^{64}Cu and ^{68}Ga for small-animal positron emission tomographic/computed tomographic (PET/CT) imaging. Two commercially available NOTA analogues, p-SCN-Bn-NOTA and NODAGA, were evaluated. The p-SCN-Bn-NOTA analogues were conjugated to Y3-TATE through β-Ala and PEG$_8$ linkages. The NODAGA chelator was directly conjugated to Y3-TATE. The analogues labeled with ^{64}Cu or ^{68}Ga were analyzed in vitro for binding affinity and internalization and in vivo by PET/CT imaging, biodistribution, and Cerenkov imaging (^{68}Ga analogues). We evaluated the effects of the radiometals, chelators, and linkers on the performance of the SSTR subtype 2-–targeted imaging agents and also compared them to a previously reported agent, ^{64}Cu-CB-TE2A-Y3-TATE. We found that the method of conjugation, particularly the length of the linkage between the chelator and the peptide, significantly impacted tumor and nontarget tissue uptake and clearance. Among the ^{64}Cu- and ^{68}Ga-labeled NOTA analogues, NODAGA-Y3-TATE had the most optimal in vivo behavior and was comparable to ^{64}Cu-CB-TE2A-Y3-TATE. An advantage of NODAGA-Y3-TATE is that it allows labeling with ^{64}Cu and ^{68}Ga, providing a versatile PET probe for imaging SSTr subtype 2–positive tumors.

SOMATOSTATIN RECEPTORS are overexpressed on a variety of human neuroendocrine tumors and have become an important target for molecular imaging. There are five receptor subtypes; somatostatin receptor subtype 2 (SSTR2) is found in a variety of malignancies and has become the target for molecular imaging radiolabeled somatostatin analogues.[1–9] Previous research has demonstrated that somatostatin analogues can be labeled directly with ^{18}F and ^{124}I or modified with bifunctional chelators, allowing the incorporation of radiometals.[10–12]

The radiometals ^{64}Cu and ^{68}Ga have desirable characteristics for use in positron emission tomographic (PET) imaging. ^{64}Cu ($T_{1/2}$ = 12.7 hours; β^+ [17.6%] 653 keV; β^- [38.4%] 579 keV) is ideal for tracers with slower accumulation within the target site and clearance from nontargeted tissues and is also a promising radiometal for radiotherapy due to β^- emission.[13] Gallium-68 ($T_{1/2}$ = 67.7 minutes; β^+ [87.7%] 1,899 keV) has become a more widely used radiometal for PET imaging due to the convenience of its production from a ^{68}Ge/^{68}Ga generator.[14] In addition, the high-energy positron emitted by ^{68}Ga has potential for Cerenkov luminescence imaging, which can be monitored using simpler and less expensive whole-animal optical imaging equipment.[15,16]

The choice of bifunctional chelator and radiometal has been shown to have a direct effect on the pharmacokinetics of SSTR-targeted imaging agents. The chelator NOTA and its analogues form stable complexes with both ^{64}Cu and ^{68}Ga.[17–19] The NOTA analogues NODAGA and p-SCN-Bn-NOTA have three carboxylates available for radiometal complexation after conjugation to peptides and proteins. Lin and colleagues demonstrated that ^{68}Ga-[Tyr^3]-octreotide modified with a NOTA analogue having three carboxylates demonstrated greater accumulation in SSTR-positive xenograft with superior pharmacokinetics than analogues with more carboxylates.[20] In addition, this analogue demonstrated pharmacokinetics akin to the DOTA analogue but with superior clearance from the liver.[20] Fani and colleagues

From the Departments of Radiology, Pharmacology & Chemical Biology, and Bioengineering, University of Pittsburgh, Pittsburgh, PA, and the Department of Radiation Oncology, Washington University, St. Louis, MO.

Address reprint requests to: Carolyn J. Anderson, PhD, Department of Radiology, University of Pittsburgh, 100 Technology Drive, Suite 452, Pittsburgh, PA 15219; e-mail: andersoncj@upmc.edu.

DOI 10.2310/7290.2014.00020

radiolabeled NODAGA-LM3, a modified somatostatin antagonist, with ^{64}Cu and ^{68}Ga and evaluated the effects of the radiometal on their in vivo performance.[21] The accumulation in the SSTR-positive xenograft was similar for both agents, but there were significant differences in the clearance from the kidneys and pancreas.

Here we compare commercially available chelators, p-SCN-Bn-NOTA and NODAGA, conjugated to the SSTR2-targeted somatostatin agonist Y3-TATE and radiolabeled with ^{64}Cu and ^{68}Ga. The rationale for comparing NOTA analogues is to determine the effect of radiometal and linkages of NOTA analogues on the in vivo performance of the agonist, Y3-TATE, as this analogue has been investigated in human studies.[22–26] The NODAGA chelator was directly conjugated to Y3-TATE, whereas the p-SCN-Bn-NOTA chelators were conjugated to Y3-TATE through β-Ala and PEG_8 linkages. The in vitro and in vivo results were compared to evaluate the effects of the radiometal, chelators, and linker. The NOTA conjugates were compared to ^{64}Cu-CB-TE2A-Y3-TATE, which previously showed high SSTR2-positive tumor uptake with clearance through nontarget tissues.[27,28]

Materials and Methods

General

^{64}Cu was purchased from Washington University School of Medicine and University of Wisconsin School of Medicine and Public Health. ^{68}Ga (Eckert & Ziegler Isotope Products, Berlin, Germany) was eluted directly to a Modular-Lab (Eckert & Ziegler Isotope Products), concentrated on a Strata-X-C column from Phenomenex (Torrance, CA), and the ^{68}Ga-eluate was collected by desorbing it with 0.8 mL of 0.01 M HCl/98% acetone solution. HCT116 cells were provided by Dr. Bert Vogelstein at Johns Hopkins University and were transfected with SStr2 as previously described.[29] S-2-(4-isothiocyanatobenzyl)-1,4,7-triazacyclononane-1,4,7-triacetic acid (p-SCN-Bn-NOTA) was purchased from Macrocyclics (Dallas, TX), and 2,2′-(7-(1-carboxy-4-((2,5-dioxopyrrolidin-1-yl)oxy)-4-oxobutyl)-1,4,7-triazonane-1,4-diyl)diacetic acid (NODAGA-NHS ester) was purchased from CheMatech (Dijon, France). All other chemicals were purchased from Sigma-Aldrich Chemical Co. (St. Louis, MO) or Fisher Scientific (Pittsburgh, PA).

Synthesis of Y3-TATE Analogues

4,11-Bis(carboxymethyl)-1,4,8,11-tetraazabicyclo[6.6.2]hexadecane (CB-TE2A) conjugated to Y3-TATE was synthesized as previously reported.[29] The general protocol for peptide synthesis of the conjugates used for this study has been previously described.[28,30] Briefly, the peptides were prepared on a solid support by standard Fmoc procedures using a preloaded Fmoc-Thr(Boc)-Wang resin. Fmoc deprotection was achieved by washing the resin with 20% piperidine DMF (five times) for 2 minutes, followed by washing the resin three times with DMF. The carboxyl group was activated using 2-(1H-benzotriazole-1-yl)-1,1,1,3-tetramethyluronium hexafluorophosphate (HBTU) and di-isopropylethylamine (DIPEA) to couple the subsequent Fmoc-protected amino acids. Cyclization of the peptide was accomplished by treating the resin with $Tl(TFA)_3$ in dimethylformamide (DMF). Following cyclization, the Fmoc was removed from D-Phe to expose the free amine. The free amine was treated under three conditions to provide the Y3-TATE analogues for this study. NODAGA-Y3-TATE was prepared by treating the resin with NODAGA-NHS (2 Eq) and N,N′-diisopropylethylamine (DIPEA) (5 Eq) in DMF overnight. NOTA-PEG_8-Y3-TATE (NOTA-PEG_8) was prepared by first treating the resin with Fmoc-PEG_8-CH_2CH_2-COOH following standard Fmoc procedures. Following the deprotection, the resulting free amine was treated with p-SCN-Bn-NOTA (1.5 Eq) and DIPEA (6 Eq) dissolved in DMF and reacted overnight. NOTA-β-Ala-Y3-TATE (NOTA-β-Ala) was prepared under the same methods as NOTA-PEG_8, with Fmoc-β-Ala used as the linker instead of Fmoc-PEG_8-CH_2CH_2-COOH. The resins were washed, the individual peptides were cleaved, and side chain–protecting groups were removed using a trifluoroacetic acid (TFA) solution (90% TFA, 5% water, 5% triisopropylsilane). The cleaved peptides were precipitated out of solution using ice-cold diethyl ether and washed twice with diethyl ether. The peptides were dissolved in 10% acetic acid and purified using preparatory high-performance liquid chromatography (HPLC), where solvent A is 0.1% TFA in water and solvent B is 0.1% TFA in acetonitrile. The HPLC purification was carried out on a Phenomenex Jupiter 5u C18 300 Å semipreparative column (250 × 10 mm, 5 microns) starting at 82% A held for 2 minutes, then a linear gradient to 65% A over 10 minutes, followed by a linear gradient to 50% over 3 minutes and a linear gradient to 10% A over 1 minute. This was held for an additional minute followed by a linear gradient to 82% A over 1 minute and held for 4 minutes. The solvent was removed in vacuo to yield pure Y3-TATE analogues. The Y3-TATE analogues (Figure 1) were characterized on a Waters e2695/ LCT Premier XE LCMS: NODAGA-Y3-TATE ($C_{64}H_{87}N_{13}O_{19}S_2$), [M] calculated 1405.5683, found 1405.4971; NOTA-PEG_8-Y3-TATE ($C_{88}H_{127}N_{15}O_{27}S_3$),

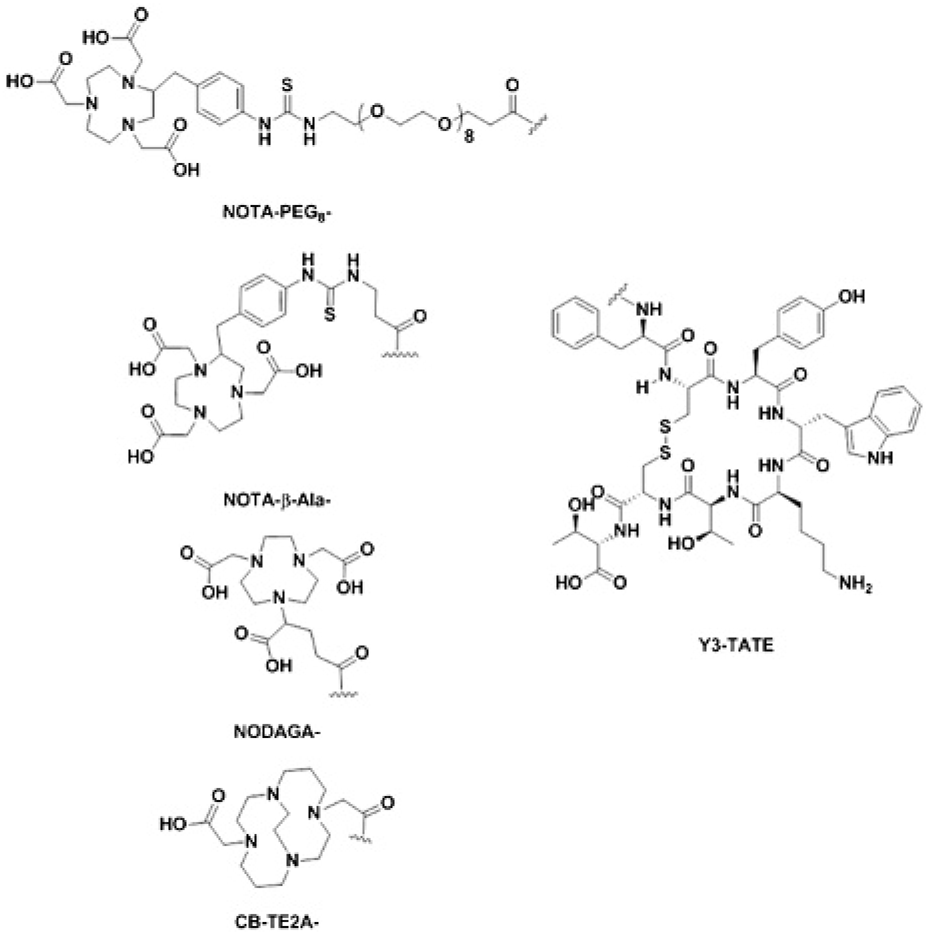

Figure 1. Structures of NOTA- and CB-TE2A-Y3-TATE analogues.

$[MH]^+$ calculated 1922.8266, found 1923.0698; NOTA-β-Ala-Y3-TATE ($C_{72}H_{95}N_{15}O_{19}S_3$), [M] calculated 1569.6091, found 1570.3997.

Synthesis of Cold Standards of Cu- and Ga-Y3-TATE Analogues

Cold copper labeling was achieved by reacting 300 μg of each of the NOTA-Y3-TATE analogues, 300 μL 10% acetic acid, and 2 mg of copper acetate for 30 minutes at 95°C. Cold gallium labeling was achieved under the same conditions using gallium trichloride. The reaction solution was purified using preparatory HPLC, where solvent A is 0.1% TFA in water and solvent B is 0.1% TFA in acetonitrile. The HPLC purification was carried out on a Phenomenex Jupiter 5u C18 300 Å semipreparative column (250 × 10 mm, 5 microns) starting at 97% A, a linear gradient to 3% A over 10 minutes, and then held for an additional 7 minutes. This was followed by a linear gradient to 97% over 1 minute and held for an additional 4 minutes. The desired peak was collected and solvent was removed in vacuo to yield pure Cu- and Ga-NOTA-Y3-TATE analogues. The Cu- and Ga-NOTA-Y3-TATE analogues were characterized on a Waters (Milford, MA) e2695/LCT Premier XE LCMS: Cu-NODAGA-Y3-TATE ($C_{64}H_{87}CuN_{13}O_{19}S_2$), [M] calculated 1467.103, found 1467.272; Ga-NODAGA-Y3-TATE ($C_{64}H_{87}GaN_{13}O_{19}S_2$), [M] calculated 1473.280, found 1473.163; Cu-NOTA-PEG$_8$-Y3-TATE ($C_{88}H_{127}CuN_{15}O_{27}S_3$), [M] calculated 1983.751, found 1983.592;Ga-NOTA-PEG$_8$-Y3-TATE ($C_{88}H_{127}GaN_{15}O_{27}S_3$), [M] calculated 1989.928, found 1989.298; Cu-NOTA-β-Ala-Y3-TATE ($C_{72}H_{95}CuN_{15}O_{19}S_3$), [M] calculated 1631.331, found 1631.794; Ga-NOTA-β-Ala-Y3-TATE ($C_{72}H_{95}GaN_{15}O_{19}S_3$), [MH]+ calculated 1636.519, found 1636.989.

Radiolabeling

^{64}Cu radiolabeling was achieved by reacting 2 to 2.5 μg of each of the Y3-TATE analogues, 200 μL 0.4 M NH_4OAc (initial pH 7.0), and ≈ 37 MBq of $^{64}CuCl_2$ in 0.1 N hydrochloric acid for 30 minutes at 95°C. The coordination of ^{68}Ga was achieved under similar conditions. Two micrograms of each Y3-TATE analogue, 200 μL 0.4 M NH_4OAc (initial pH 7.0) and ≈ 37 MBq of $^{68}GaCl_3$ in 0.1 N hydrochloric acid/98% acetone solution were reacted for 30 minutes at 95°C in an open vial. ^{64}Cu-CB-TE2A-Y3-TATE was prepared as previously described.[28] Quality control of the radiolabeled peptides was performed on a Waters 2489/1525 HPLC to determine radiolabeling yield.

Receptor Binding Assays

Membrane preparations of HCT116-SSTr2 cells were used for binding assays, and assays were performed on Perkin-Elmer Unifilter (Waltham, MA) 96-well, GF/B filtration plates using previously described methods, with some modifications.[28,29,31] Membranes were diluted in binding buffer (50 mM Tris-hydrochloride [pH 7.4]; 5 mM $MgCl_2 \cdot 6\ H_2O$; 0.1% bovine serum albumin; and 0.5 mg of aprotinin, 200 mg of bacitracin, 10 mg of leupeptin, and 10 mg of pepstatin A per milliliter), and 15 μg of membrane protein was used per well. Increasing concentrations of ^{64}Cu-labeled Y3-TATE analogues were added to membranes to measure total binding, and nonspecific binding was determined by conducting the assay in the presence of an excess of Y3-TATE. After incubation of the membranes at room temperature for 2 hours, the medium was removed and the membranes were washed twice with 200 μL of binding buffer. OptiPhase Super-Mix (50 μL; PerkinElmer, Waltham, MA) was added to each well, and bound activity was measured with a liquid scintillation and luminescence counter (2450 Microbeta^2, PerkinElmer). All dissociation constant (K_d) values were estimated from nonlinear curve fitting of bound peptide versus the sum of the concentrations of ^{64}Cu-Y3-TATE analogues and Y3-TATE using *Prism* software (GraphPad, La Jolla, CA).

Competitive Binding Assay

Receptor binding affinities (K_i) of cold Cu- and Ga-labeled NOTA-Y3-TATE analogues were calculated from half-maximal inhibitory concentration (IC_{50}) values determined by a competitive binding assay using ^{64}Cu-NODAGA-Y3-TATE. Assays were performed on Unifilter 96-well, GF/B filtration. Plates were prepared by adding the following, as ordered, to each well: binding buffer, varying concentrations of cold Cu- or Ga-NOTA-Y3-TATE analogues (0–1,000 nM), ^{64}Cu-NODAGA-Y3-TATE (final concentration 0.5 nM), and 15 μg of membrane protein. Membranes and binding buffer were prepared as stated above in the receptor binding assay. The plates were allowed to incubate for 3 hours at room temperature (incubation time was four times the K_{off} of ^{64}Cu-NODAGA-Y3-TATE; data not shown). The cells were then washed twice with phosphate-buffered saline, OptiPhase Super-Mix (50 μL; PerkinElmer) was added to each well, and bound activity was measured with a liquid scintillation and luminescence counter (2450 Microbeta^2). The IC_{50} values were calculated by fitting the quadruplicate data with nonlinear regression using GraphPad *Prism* software. The Ki values were calculated by using the Cheng-Prusoff equation.[32]

Internalization Studies

Internalization studies were performed as previously described.[27] Briefly, HCT116-SSTr2 cells were cultured in McCoy's 5A medium supplemented with 10% fetal bovine serum, 1% pencillin-streptomycin-glutamine, and Zeocin (1 μg/mL); cells were incubated at 37°C in a humidified 5% CO_2 atmosphere. Before each assay, aliquots of prepared 2×10^7 cells/mL were placed in a 12-well plate and incubated overnight. The wells were prepared as previously described,[27] and ^{64}Cu-labeled Y3-TATE analogues (6 ng/10 μL) were added to blocked and unblocked wells ($n = 3$). Blocked wells were pretreated with 2 μg/10 μL of Y3-TATE and washed, and new growth medium was added. The cells were allowed to incubate for 10 minutes at 37°C. Following incubation, the medium was collected in separate fractions; the surface bound and the lysed cells were counted on a Packard Cobra II automated gamma counter (Packard Instrument Company, Downers Grove, IL). The total protein concentration in the cell lysate was determined using the BCA Protein Assay (Pierce Biotechnology, Rockford, IL). Internalized and surface-bound fractions were expressed as fmol/mg of protein.

Biodistribution

All animal studies were conducted under protocols approved by the University of Pittsburgh and Washington University Institutional Animal Care and Use Committees (IACUC). Biodistribution experiments were conducted as previously described with some modifications.[31] Briefly, healthy NCr nude female mice (6–8 weeks, Taconic Labs, Hudson, NY) bearing HCT116-SSTR2-positive tumors were injected with ^{64}Cu- and ^{68}Ga-Y3-TATE analogues (0.74–1.85 MBq) via the tail vein. Animals were sacrificed at selected time points following the injection, and organs of interest were removed, weighed, and counted on a WIZARD^2 gamma counter (PerkinElmer). In addition, blocking studies were performed for ^{64}Cu analogues at 4 hours where the mice were injected with 50 μg of Y3-TATE

30 minutes prior to injection of the radiotracer, except CB-TE2A-Y3-TATE, which was coinjected with 100 μg of Y3-TATE at 4 hours. The percent injected dose per gram (%ID/g) was calculated by comparison to a weighed, diluted standard.

PET/CT Imaging

Imaging studies were performed using NCr nude female mice (6–8 weeks, Taconic Labs) bearing HCT116-SSTR2 tumors either in the shoulder or flank. Mice were injected with the ^{64}Cu- and ^{68}Ga-labeled Y3-TATE analogues (3.7–8.4 MBq) via the tail vein. After probe injection, imaging was performed at the following time points: ^{68}Ga probes = 1 hour, ^{64}Cu probes = 1 and 4 hours. For tail vein injection and throughout imaging, the mice were anesthetized with 2 to 3% isoflurane under oxygen at a flow rate of 2 L/min. PET/CT imaging was performed on an Inveon small-animal PET/CT scanner (Siemens Molecular Imaging, Knoxville, TN) with the following parameters: 600-second PET acquisition time, two-dimensional (2D) ordered subset expectation maximization (OSEM) (standard uptake value [SUV] calculations) and three-dimensional (3D) OSEM (PET/CT images) reconstruction algorithms, CT-based attenuation correction, voxel size 0.7 mm^3; CT exposure settings: 80 kV, 500 mA, 120 ms exposure time, 220° rotation with 120 steps, low magnification, bin 4, voxel size 0.8 mm^3; CT reconstruction: Shepp-Logan reconstruction filter, bilinear interpolation, downsample factor 2, voxel size: x = 412.9 μm, y = 412.9 μm, z = 533.33 μm. ^{64}Cu-CB-TE2A-Y3-TATE was imaged as previously described at 2 hours postinjection.[27,33,34] All PET images were manually coregistered to the CT, analyzed, and prepared using the *Inveon Research Workplace* software (Siemens Molecular Imaging). PET images were exported as maximum intensity projections, and final images were prepared using *ImageJ* software (National Institutes of Health [NIH], Bethesda, MD) and Adobe *Photoshop* CS5.

Cerenkov Luminescence Imaging

Following PET/CT imaging, mice injected with ^{68}Ga-based probes were placed into an IVIS Lumina XR optical imaging station (PerkinElmer) to evaluate Cerenkov luminescence in the tumors. Images were acquired using the following parameters: no light acquisition filter, acquisition time: 300 seconds, binning: 8 × 8, F/stop: 1, field of view: 10 cm × 10 cm. Animals were anesthetized with 2% isoflurane under oxygen with a flow rate of 2 L/min throughout imaging and were heated by a 37°C platform throughout imaging. Machine control was performed using *Living Image* software version 3.1 (PerkinElmer). The 16-bit TIFF output images were opened using *ImageJ* software, and outlier hotspots due to cosmic radiation were removed using the "remove outliers" tool. Images were then background subtracted using the rolling ball algorithm (radius = 500 pixels). Free-hand regions of interest (ROI) were drawn around the tumor and the leg opposite the tumor as a muscle reference, and mean pixel intensities were measured within each ROI. Tumor to muscle ratios were then calculated. Image labels were added using Adobe *Photoshop* CS5.

Statistical Analysis

Prism version 5 software was used to determine *p* values and statistical significance. An unpaired *t*-test was used to compare biodistribution values presented in this article.

Results

Synthesis and Radiolabeling

Y3-TATE was prepared on resin as previously described.[28,30] The terminal D-Phe was deprotected on the resin to expose the free amine for incorporation of the NOTA chelators and linkers. The free amine was modified to provide the chelator-Y3-TATE analogues in the following yields: NODAGA-Y3-TATE (1.9%), NOTA-β-Ala-Y3-TATE (2.1%), and NOTA-PEG_8-Y3-TATE (3.4%). These analogues were radiolabeled in high yield and purity with ^{64}Cu (≥ 95%) and ^{68}Ga (≥ 99%). The specific activities ranged between 42.2 and 150.6 MBq/μmol (Table 1).

Receptor Binding Assays

A saturation binding assay was performed using HCT116-SSTR2 membranes.[31] The dissociation constant (K_d) for ^{64}Cu-NODAGA-Y3-TATE (0.5 ± 0.1 nM) was similar to the previously reported values for ^{64}Cu-CB-TE2A-Y3-TATE (Table 2)[29]; however, the B_{max} was greater for the CB-TE2A analogue compared to the NODAGA analogue (4200 ±

Table 1. Specific Activities (GBq/μmol) of NOTA Analogues at End of Bombardment (^{64}Cu) and End of Elution (^{68}Ga)

	^{64}Cu	^{68}Ga
NODAGA-Y3-TATE	91.2–110.0	42.2–44.9
NOTA-β-Ala-Y3-TATE	115.8–150.6	56.5–68.7
NOTA-PEG_8-Y3-TATE	84.0–125.9	81.0–102.1

200 vs 2048 ± 79.9 fmol/mg, respectively). Linker modifications to p-SCN-Bn-NOTA significantly decreased the affinity of the radiotracers (β-Ala analogue 1.8 ± 0.7 nM; PEG_8 analogue: 2.3 ± 0.9 nM; $p \leq .05$); in addition, increasing the size of the linker resulted in lower B_{max} values. The use of the β-Ala linker demonstrated a slightly lower B_{max} (1660 ± 190 fmol/mg) to the linker free NODAGA analogue, whereas the use of the PEG_8 linker greatly reduced the B_{max} (980 ± 130 fmol/mg); $p \leq .05$).

Competitive Binding Assays

The IC_{50} values were determined in a competitive binding assay using ^{64}Cu-NODAGA-Y3-TATE as the radioligand and HCT116-SSTR2 membranes (see Table 2). The competitive binding assays were performed once, and the Ki value was calculated from the IC_{50} using the Cheng-Prusoff equation. Cu- and Ga-NODAGA-Y3-TATE presented the lowest K_i values for the NOTA analogues; both analogues had a K_i of 0.6 nM. As seen with the dissociation constants, the addition of linkers demonstrated an increase in the K_i values. For the β-Ala linker, the cold Cu analogue had a K_i of 1.5 nM, which was slightly lower than the Ga analogue, with a K_i of 4.0 nM. The difference between the Cu- and Ga-NOTA analogues was the greatest for NOTA-PEG_8-Y3-TATE: Cu-NOTA-PEG_8-Y3-TATE (K_i = 16 nM) and Ga-NOTA-PEG_8-Y3-TATE (K_i = 2.5 nM).

Internalization Studies

Internalization studies were performed with HCT116-SSTR2 cells (Figure 2). ^{64}Cu-NOTA-PEG_8-Y3-TATE demonstrated rapid internalization within 30 minutes, slightly increasing over 4 hours (3460 ± 130 fmol/mg). Unlike ^{64}Cu-NOTA-PEG_8-Y3-TATE, the internalization of the β-Ala and NODAGA analogues continued to significantly increase over the 4-hour window, ^{64}Cu-NOTA-β-Ala-Y3-TATE by 49% and ^{64}Cu-NODAGA-Y3-TATE by 59% from the initial 15-minute time point. The addition of the blocking agent at each time point reduced the uptake of all ^{64}Cu-labeled NOTA-Y3-TATE analogues, indicating that the internalization was receptor mediated.

Biodistribution

Biodistribution studies were carried out in NCr nude female mice (6–8 weeks) bearing HCT116-SSTR2 tumors. At 1 hour, all ^{64}Cu and ^{68}Ga analogues had high uptake in the kidneys, pancreas, and SSTR2-positive tumors (Figure 3 and Figure 4). At 1 hour, the ^{64}Cu- and ^{68}Ga-labeled compounds showed significant differences in kidney uptake. The Ga-labeled NOTA analogues demonstrated higher kidney uptake compared to the Cu-labeled analogues, with the exception of the NODAGA-Y3-TATE. The uptake in the pancreas for all analogues decreased to background by 24 hours. Compared to the ^{64}Cu- and ^{68}Ga-labeled NODAGA and PEG_8 analogues, the ^{64}Cu- and ^{68}Ga-labeled NOTA-β-Ala-Y3-TATE analogues exhibited significantly higher uptake in the pancreas at 1 hour (p values ≤ .05), which decreased by 4 hours, presenting uptake similar to that of the other analogues. Although the ^{68}Ga-NOTA analogues had greater %ID/g values at 1 hour compared to the analogous ^{64}Cu compounds, the differences were not statistically significant (p values ≥ .1).

At 4 hours, ^{64}Cu-NODAGA-Y3-TATE and ^{64}Cu-CB-TE2A-Y3-TATE demonstrated significantly higher uptake in the tumor (15 ± 4.8% and 13 ± 3.1 %ID/g) than both the PEG_8 and β-Ala analogues (5.5 ± 1.7 and 5.8 ± 2.6 %ID/g; $p < .01$). At 24 hours, ^{64}Cu-NOTA-PEG_8-Y3-TATE (5.2 ± 1.2 %ID/g; $p < .03$) presented with the highest tumor uptake, but uptake in the kidneys and liver was greater than in the CB-TE2A, NODAGA, and β-Ala analogues. ^{64}Cu-NODAGA-Y3-TATE and ^{64}Cu-CB-TE2A-Y3-TATE at 24 hours had the highest tumor uptake (3.3 ± 0.5 %ID/g; 3.3 ± 0.3 %ID/g),

Table 2. Dissociation Constant, B_{max} and Binding Affinity of NOTA and CB-TE2A Analogs

	Copper-64		*Copper**		*Gallium**	
	K_d *(nM)*	B_{max} *(fmol/mg)*	K_i *(nM)*	*95% CI*	K_i *(nM)*	*95% CI*
NODAGA-Y3-TATE	0.5 ± 0.1	2050 ± 80	0.6	0.3–1.3	0.6	0.2–2.4
NOTA-β-Ala-Y3-TATE	1.8 ± 0.7	1660 ± 186	1.5	0.1–30	4.0	0.1–195
NOTA-PEG_8-Y3-TATE	2.3 ± 0.9	984 ± 126	2.5	0.1–53	16	3.1–87
CB-TE2A-Y3-TATE†	0.5 ± 0.1	4200 ± 200	N/A			

N/A = not available.
*Ki assays were preformed once with the cold standards of the NOTA-Y3-TATE analogues.
†Previously reported.[29]

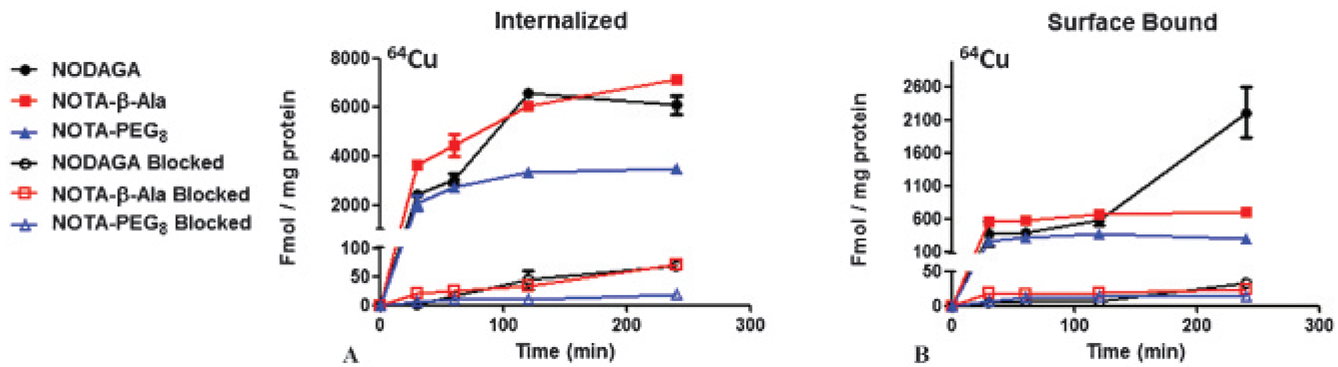

Figure 2. Internalization studies performed with ^{64}Cu-labeled NOTA-Y3-TATE analogues using HCT116-SSTR2-positive colorectal carcinoma cells (n = 3). Blocking was achieved with cold Y3-TATE (n = 3). (A) Internalized and (B) surface-bound ^{64}Cu-NOTA-Y3-TATE analogues in HCT116-SSTR2-positive cells with and without blocking.

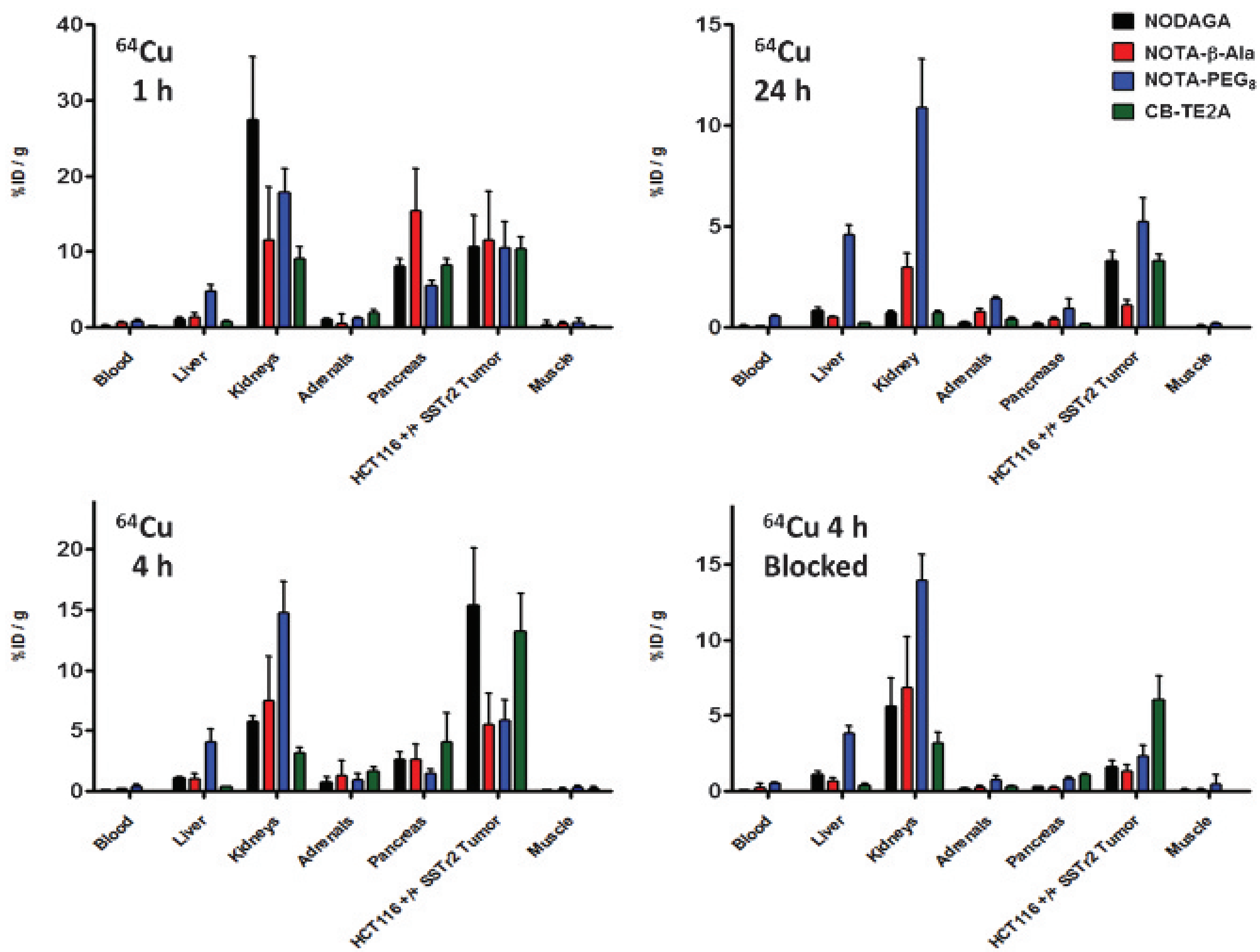

Figure 3. Biodistribution of ^{64}Cu-NOTA and CB-TE2A-Y3-TATE analogues at 1 hour, 4 hours, 4 hours blocked, and 24 hours in NCr nude mice bearing HCT116-SSTR2 tumors (n = 4 for each group).

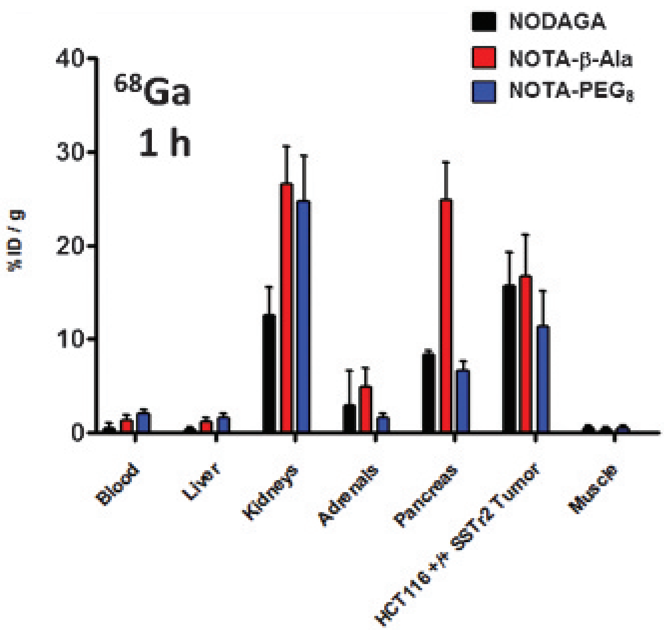

Figure 4. Biodistribution of ^{68}Ga-NOTA-Y3-TATE analogues at 1 hour in NCr nude mice bearing HCT116-SSTR2-positive tumors (n = 4 for each group).

with significant clearance from nontargeted organs. At 24 hours, ^{64}Cu-NOTA-β-Ala-Y3-TATE showed the highest uptake in the kidneys (3.0 ± 0.3 %ID/g), followed by the tumor (1.1 ± 0.3 %ID/g).

Of all compounds evaluated, ^{64}Cu-NODAGA-Y3-TATE demonstrated superior tumor to blood/muscle ratios for all time points; however, at 1 hour, the tumor to blood/muscle ratio of ^{64}Cu-NODAGA-Y3-TATE and the tumor to muscle ratios of all the ^{64}Cu-labeled NOTA analogues at 4 hours were not statistically significant ($p \geq .07$) compared to ^{64}Cu-CB-TE2A-Y3-TATE (Table 3). For the NOTA analogues, ^{68}Ga- and ^{64}Cu-labeled NODAGA-Y3-TATE provided the highest tumor to blood/muscle ratios. The tumor to muscle and tumor to blood ratios for the ^{64}Cu-labeled analogues were highest at 4 hours with the exception of NOTA-PEG$_8$-Y3-TATE, where the tumor to muscle/blood ratios were similar at 1 and 4 hours (see Table 3). ^{64}Cu-CB-TE2A-Y3-TATE demonstrated the highest tumor to muscle/blood ratios of all the analogues at 1 hour (74 ± 25 and 120 ± 60, respectively). Of the NOTA analogues at 1 hour, ^{64}Cu-NODAGA-Y3-TATE demonstrated the highest tumor to muscle/blood (73 ± 78 and 58 ± 26, respectively); however, it should be noted that the differences in tumor to muscle ratios are not statistically significant.

Blocking with unlabeled Y3-TATE demonstrated a reduction in SSTR2-targeted agents for all compounds. Preblocking caused a 90% decrease in tumor uptake of ^{64}Cu–NODAGA-Y3-TATE (1.8 ± 0.5 %ID/g), a 76% decrease in ^{64}Cu-NOTA-β-Ala-Y3-TATE (1.3 ± 0.4 %ID/g), and a 61% decrease in ^{64}Cu-NOTA-PEG$_8$-Y3-TATE (2.3 ± 0.8 %ID/g). ^{64}Cu-CB-TE2A-Y3-TATE (6.1 ± 1.6 %ID/g) was coinjected with Y3-TATE but still demonstrated reduced uptake in the tumor by 54%. The decrease in tumor uptake when preinjected or coinjected with Y3-TATE indicates selective binding of SSTR2 for all analogues.

PET/CT Imaging

The PET/CT images for all the ^{64}Cu and ^{68}Ga Y3-TATE analogues evaluated in this study (n = 2) had high contrast for the tumor along with no-target uptake in kidneys and bladder (Figure 5 and Figure 6), except ^{68}Ga-NOTA-PEG$_8$-Y3-TATE (n = 1), which had low contrast to nontarget uptake. The nontarget uptake in the kidneys and bladder is due to clearance of the PET agents. In comparing the ^{64}Cu- or ^{68}Ga-labeled analogues, it should be noted that there were no significant differences in the SUV and tumor to muscle ratios. The SUVs ranged between 0.48 and 4.0, with ^{64}Cu-NOTA-β-Ala-Y3-TATE demonstrating the highest SUV at 1 hour (4.0 ± 0.6), and this agent and ^{64}Cu-NODAGA-Y3-TATE had the

Table 3. Biodistribution Tumor to Blood/Muscle Ratios of NOTA and CB-TE2A Y3-TATE Analogues in HCT116 SSTR2-Positive Tumor-Bearing Mice at 1, 4, and 24 Hours (n = 4 for each group)

	^{68}Ga, 1 h		*^{64}Cu, 1 h*		*^{64}Cu, 4 h*		*^{64}Cu, 24 h*	
Tumor to	*Blood*	*Muscle*	*Blood*	*Muscle*	*Blood*	*Muscle*	*Blood*	*Muscle*
NODAGA-Y3-TATE	42 ± 34	54 ± 43	58 ± 26*	73 ± 78*	90 ± 39	195 ± 57*	36 ± 2	100 ± 15
NOTA-β-Ala-Y3-TATE	14 ± 6†	53 ± 29†	18 ± 3	27 ± 16	30 ± 9	58 ± 39*	13 ± 3	28 ± 15
NOTA-PEG$_8$-Y3-TATE	5.8 ± 2†	28 ± 18†	13 ± 4	32 ± 23	14 ± 1	31 ± 20*	10 ± 3	29 ± 11
CB-TE2A-Y3-TATE	N/A	N/A	74 ± 25	120 ± 60	251 ± 58	220 ± 173	122 ± 18	366 ± 225

N/A = not available.
*Not statistically significant (p values ≥ .07) compared to ^{64}Cu "gold standard," ^{64}Cu-CB-TE2A-Y3-TATE.
†Not statistically significant (p values ≥ .07) compared to ^{68}Ga-NODAGA-Y3-TATE.

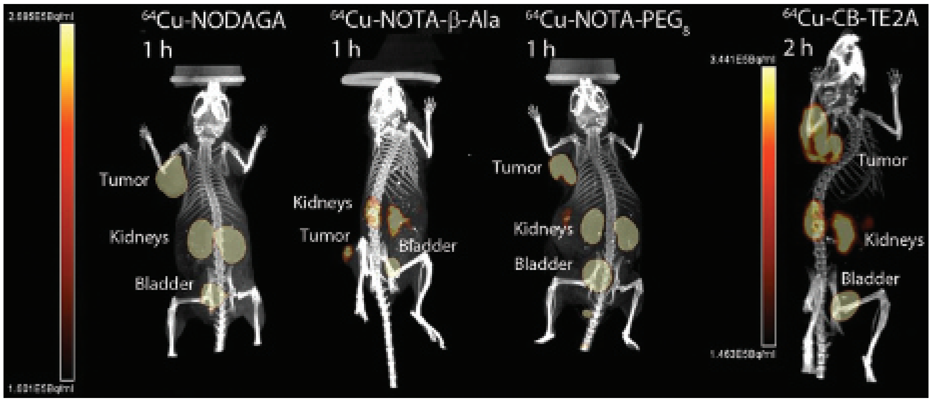

Figure 5. PET/CT images of ^{64}Cu-NOTA-Y3-TATE analogues 1 hour postinjection: NODAGA (6.1 MBq), NOTA-β-Ala (2.4 MBq), NOTA-PEG$_8$ (4.2 MBq). PET/CT image of ^{64}Cu-CB-TE2A-Y3-TATE 2 hours postinjection (7.2 MBq). PET/CT images were performed with NCr nude mice bearing HCT116-SSTR2 tumors. Images are maximum intensity projections and rotated to achieve the best presentation of the tumor.

highest SUVs at 4 hours (3.1 ± 0.5 and 3.1 ± 0.9) (Table 4). The ^{64}Cu-labeled β-Ala and PEG$_8$ NOTA-Y3-TATE analogues demonstrated lower SUVs at 1 hour compared to the NODAGA conjugate. ^{64}Cu-NODAGA-Y3-TATE demonstrated the second highest SUV (3.1 ± 1.3) at 1 hour, whereas ^{64}Cu-labeled NOTA-β-Ala-Y3-TATE (4.0 ± 0.6) had the highest, followed by the NODAGA, NOTA-PEG$_8$ (2.6 ± 0.6), and CB-TE2A (2.2 ± 0.6) analogues. At 1 hour, the tumor to muscle trend was as follows: ^{64}Cu-NODAGA-Y3-TATE (324 ± 438) demonstrated the highest, followed by ^{64}Cu-CB-TE2A-Y3-TATE (34 ± 16), ^{64}Cu-NOTA-β-Ala-Y3-TATE (13 ± 5.0), and ^{64}Cu-PEG$_8$-Y3-TATE (8.9 ± 1.6). At 4 hours, the trend reversed for the NOTA analogues, with ^{64}Cu-PEG$_8$-Y3-TATE (38 ± 3.4) having the highest and ^{64}Cu-NODAGA-Y3-TATE (26 ± 2.1) the lowest.

^{68}Ga-NODAGA-Y3-TATE demonstrated the highest SUV of the ^{68}Ga-labeled analogues (2 ± 0.14). ^{68}Ga-NODAGA-Y3-TATE and ^{68}Ga-NOTA-PEG$_8$-Y3-TATE (n = 1) had similar tumor to muscle ratios compared to ^{68}Ga-NOTA-β-Ala-Y3-TATE (18 ± 4.3, 15 and 9 ± 7.2, respectively). ^{68}Ga-NOTA-PEG$_8$-Y3-TATE showed the lowest tumor uptake of all compounds (SUV = 0.5, n = 1; see Figure 6); however, the ^{64}Cu agent had higher uptake at 1 and 4 hours (2.6 ± 0.6 and 1.9 ± 0.4; see Figure 5).

Cerenkov Imaging

To demonstrate the multimodal imaging utility of the three ^{68}Ga-based probes, the HCT116-SSTR2-positive mice were also imaged by Cerenkov imaging in the bioluminescence imaging scanner from 1.5 to 2 hours following PET/CT. In mice imaged with ^{68}Ga-NODAGA-Y3-TATE, the tumor images showed good contrast with minimal background other than the kidneys (Figure 7). Due to the semiquantitative nature of this 2D technique, exact values of uptake could not be calculated, but tumor to muscle ratios were measured through ROI analysis of the planar images generated by the Cerenkov emissions. Following the same trend as PET imaging at 1 hour, ^{68}Ga-NODAGA-Y3-TATE showed a greater tumor to muscle ratio than ^{68}Ga-NOTA-β-Ala-Y3-TATE and ^{68}Ga-NOTA-PEG$_8$-Y3-TATE (11 ± 4, 4.4 ± 7, and 4.4 [n = 1]). It should be noted that Cerenkov imaging was not attempted on mice injected with ^{64}Cu-based probes, because the lower beta energy copper emissions produce significantly

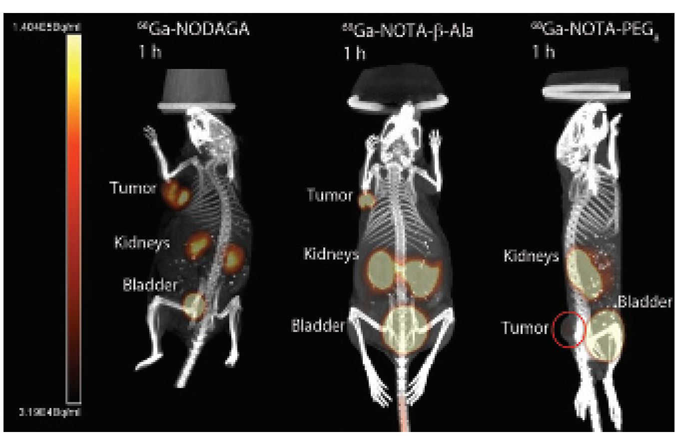

Figure 6. PET/CT images of ^{68}Ga-NOTA-Y3-TATE analogues 1 hour post-injection: NODAGA (5.2 MBq), NOTA-β-Ala (4.6 MBq), NOTA-PEG$_8$ (6.8 MBq). PET/CT images were performed with NCr nude mice bearing HCT116-SSTR2 tumors. Images are maximum intensity projections and rotated to achieve the best presentation of the tumor; in the ^{68}Ga-NOTA-PEG$_8$-Y3-TATE image, the tumor is circled due to high activity in the bladder.

Table 4. PET/CT Data of ^{68}Ga and ^{64}Cu NOTA-Y3-TATE and CB-TE2A-Y3-TATE Analogues in HCT116 SSTR2-Positive Tumor-Bearing Mice (*n* = 2 per group unless otherwise noted)

	^{68}Ga 1 h		^{64}Cu 1 h		^{64}Cu 4 h	
	SUV	*T:M*	*SUV*	*T:M*	*SUV*	*T:M*
NODAGA-Y3-TATE	2.0 ± 0.1	18 ± 4.4	3.1 ± 1.3	324 ± 438	3.1 ± 0.8	26 ± 2.1
NOTA-β-Ala-Y3-TATE	0.81 ± 1.0	8.5 ± 7.2	4.0 ± 0.6	13 ± 4.9	3.1 ± 0.5	29 ± 34
NOTA-PEG_8-Y3-TATE*	0.48	15	2.6 ± 0.6	8.9 ± 1.6	1.9 ± 0.4	38 ± 3.4
CB-TE2A-Y3-TATE†	N/A	N/A	2.2 ± 0.6†	34 ± 16†	N/A	N/A

N/A = not available; PET/CT = positron emission tomography/computed tomography; SUV = standardized uptake value; T:M = tumor to muscle ratio.
*^{68}Ga image analysis, *n* = 1.
†PET/CT performed at 2 hours.

less Cerenkov luminescence, and is not optimal for this application.

Discussion

The choice of bifunctional chelator, linker between the chelator and targeting molecule, and radiometal impacts the performance of SSTR-targeted imaging agents. This study focused on the incorporation of NOTA chelators to Y3-TATE, a well-characterized agonist of SSTR2, in comparison with CB-TE2A-Y3-TATE, which we previously showed to have high image contrast for imaging a SSTR2-positive tumor-bearing rat model.[27,28] The NOTA chelator was selected due to its ability to stably incorporate both ^{64}Cu and ^{68}Ga. In addition, NODAGA and p-SCN-Bn-NOTA are commercially available analogues of NOTA that when conjugated provide three carboxylates for N_3O_3 coordination.[17–19,35–37] The NODAGA chelator was conjugated directly to the N-terminus of Y3-TATE, resulting in an amide bond. NODAGA-Y3-TATE was previously synthesized, labeled with ^{68}Ga in high specific activity, and evaluated in Rhesus monkey brain sections[38,39]; however, to our knowledge, ^{68}Ga- or ^{64}Cu-labeled NODAGA-Y3-TATE has not been evaluated in vivo, although NODAGA has been evaluated with the SSTR2 antagonist LM3.[21] In a previously reported study, ^{64}Cu-labeled NODAGA and CB-TE2A conjugates of the SSTR2 antagonist LM3 were compared, and the NODAGA analogue was deemed superior. One of the goals of this study was to determine if this trend was similar for the widely used SSTR2 agonist Y3-TATE. In addition, we compared these agents to other NOTA-Y3-TATE conjugates and evaluated them in an SSTR2-transfected human cell line, SSTR2-positive HCT116,[29] which can be readily grown in nude mice and is a convenient model for evaluating new radiolabeled SSTR2-targeted agents.

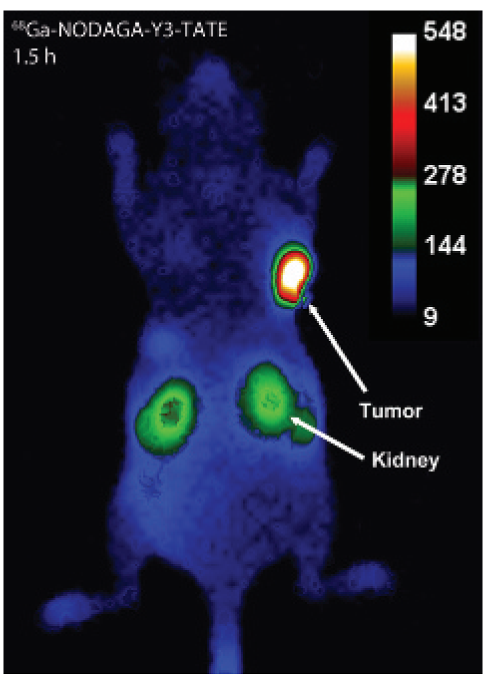

Figure 7. Cerenkov imaging 1.5 hours postinjection of ^{68}Ga-NODAGA-Y3-TATE (3.9 MBq) in NCr nude mice bearing HCT116-SSTR2 tumors. Images were acquired for 300 seconds with binning: 8 × 8, F/stop: 1, field of view: 10 cm × 10 cm. The ^{68}Ga-NODAGA-Y3-TATE Cerenkov image was selected due to its superior contrast between the tumor and background compared to the β-Ala and PEG_8 analogues.

The p-SCN-Bn-NOTA chelate was conjugated using two different linker groups; the linkers are necessary due to the instability of the thiourea bond at the α-amine. The placement of a thiourea directly on the α-amine of a peptide can cause an Edman's degradation, resulting in removal of the terminal amino acid.[40,41] The movement of the thiourea away from the α-amine can increase the stability of the thiourea when conjugated to a peptide. Banks and Paquette demonstrated that the conjugation through the ε-amine of a lysine versus the α-amine was more stable after 10 days at 37°C.[42] Cooper and colleagues demonstrated that p-SCN-Bn-NOTA conjugated through the side chain on lysine forms a stable thiourea bond with no difference in the in vivo stability compared to an amide conjugated chelator.[19] The β-Ala was selected to maintain a probe similar in size to the NODAGA and CB-TE2A analogues, whereas the PEG_8 linker was selected to analyze the effects of linker length on the probe's performance.

The ^{64}Cu analogues were evaluated in vitro by saturation binding, competitive binding, and internalization assays using HCT116-SSTR2-positive cells. ^{64}Cu/Cu-NODAGA-Y3-TATE (K_d = 0.5 ± 0.1 nM; K_i = 0.6 nM) demonstrated the highest binding affinity, similar to ^{64}Cu-CB-TE2A-Y3-TATE (K_d = 0.5 ± 0.1 nM). The addition of p-Bn-SCN-NOTA through the β-Ala and PEG_8 linkages decreased the affinity slightly (K_d = 1.8 ± 0.7 nM [K_i = 1.5 nM] and K_d = 2.3 ± 0.9 nM [K_i = 2.5 nM], respectively). The effect of the linker on affinity is mirrored in the cold gallium analogues as well: Ga-NODAGA-Y3-TATE (K_i = 0.6 nM), Ga-NOTA-β-Ala-Y3-TATE (K_i = 4.0 nM), and Ga-NOTA-PEG_8-Y3-TATE (K_i = 16 nM). Similar to the results presented here, Rogers and colleagues noted a decrease in affinity with a PEGylated bombesin analogue compared to analogues with a smaller linker.[43] Furthermore, the increase in linker length resulted in a reduced number of binding sites (B_{max}) of the ^{64}Cu-labeled analogues. We hypothesize that the larger PEG linkage created steric hindrance for binding of additional Y3-TATE-targeted agents by blocking potential binding pockets of SSTR2. ^{64}Cu-NOTA-PEG_8-Y3-TATE had the lowest B_{max}, whereas the B_{max} of ^{64}Cu-NODAGA-Y3-TATE and ^{64}Cu-NOTA-β-Ala-Y3-TATE were comparable. However, the B_{max} of ^{64}Cu-CB-TE2A-Y3-TATE was twofold higher than both analogues. ^{64}Cu-NOTA-PEG_8-Y3-TATE also demonstrated the lowest uptake and internalization in SSTR2-transfected HCT116 cells, with ^{64}Cu-NODAGA-Y3-TATE and ^{64}Cu-NOTA-β-Ala-Y3-TATE having similar, more superior internalization profiles. The in vitro results suggest that the linker length between the chelator and the peptide had an impact on their binding affinity and number of bound receptor sites. The use of the smaller β-Ala linker to maintain a similar linker length between the chelator and peptide when compared to direct conjugation appeared to have little to no effect on the in vitro performance of the radiotracers.

Based on the in vitro results we expected that the in vivo performance of NODAGA-Y3-TATE, NOTA-β-Ala-Y3-TATE, and CB-TE2A-Y3-TATE would be similar, whereas larger NOTA-PEG_8-Y3-TATE would be less optimal. The tumor uptake and nontargeted organ clearance of ^{64}Cu-NODAGA-Y3-TATE and ^{64}Cu-CB-TE2A-Y3-TATE were comparable; however, ^{64}Cu-CB-TE2A-Y3-TATE had a higher tumor to blood ratio at 4 hours. ^{64}Cu-CB-TE2A-Y3-TATE demonstrated superior tumor to muscle/blood ratios over the NOTA analogues in the biodistribution studies at 1, 4, and 24 hours, except at 1 hour, where the tumor to blood/muscle ratio of ^{64}Cu-NODAGA-Y3-TATE and all tumor to muscle ratios of ^{64}Cu-labeled NOTA analogues at 4 hours were not statistically significant ($p \geq .07$). When comparing ^{64}Cu-NODAGA-Y3-TATE and ^{64}Cu-CB-TE2A-Y3-TATE to the -β-Ala and -PEG_8 p-SCN-NOTA analogues, it is clear that the length of the linker significantly affected the in vivo performance. The increased linker length of ^{64}Cu-NOTA-PEG_8-Y3-TATE likely resulted in significantly higher ($p \leq .05$) uptake in the tumor at the 24-hour time point but with higher accumulation in the kidneys and liver at the 4- and 24-hour time points compared to the other analogues. The use of a small linker in ^{64}Cu-NOTA-β-Ala-Y3-TATE demonstrated tumor uptake comparable to ^{64}Cu-NODAGA-Y3-TATE and ^{64}Cu-CB-TE2A-Y3-TATE at 1 hour; however, washout from the tumor occurred rapidly, with a significant reduction in tumor uptake at 4 and 24 hours. The superior in vivo performances of the similar-sized ^{64}Cu-NODAGA-Y3-TATE and ^{64}Cu-CB-TE2A-Y3-TATE suggest that direct conjugation of Y3-TATE to the α-amine provides a favorable interaction with SSTr2, resulting in increased uptake and retention in the SSTR2 tumor. This is further supported by the performance of the α-conjugated ^{68}Ga-NODAGA-Y3-TATE, which had superior tumor to muscle/blood ratios in the biodistribution studies and tumor to muscle ratios in both PET/CT and Cerenkov imaging when compared to the -β-Ala and -PEG_8 analogues. It should be noted that there were significant differences between the ^{64}Cu- and ^{68}Ga-labeled analogues with respect to the kidney uptake. We hypothesize that this is a result of differences in the overall charge of these chelated metals (^{64}Cu: −1; ^{68}Ga: neutral). The differences in the kidney uptake should be considered when selecting an imaging agent to minimize the radiation dose delivered to the kidneys. Finally, the choice of the radiometals (^{64}Cu and ^{68}Ga) with the exception of kidney uptake in the evaluation of the Y3-TATE analogues through biodistribution studies, PET/CT, and Cerenkov imaging did not demonstrate a significant impact on in vivo performance of the NOTA analogues.

Conclusion

Commercially available analogues of NOTA were investigated for radiolabeling with ^{64}Cu and ^{68}Ga for SSTR2-targeted PET/CT imaging. The size and method of conjugation had a greater impact on the performance of these SSTR2-targeted PET agents than changes in radiometal, which were determined insignificant. Direct conjugation of a NOTA chelator to the α-amine of Y3-TATE (NODAGA-Y3-TATE) demonstrated superior in vivo performance for ^{64}Cu- and ^{68}Ga-labeled analogues compared to the chelator conjugated through a linker. The in vivo performance of ^{64}Cu-NODAGA-Y3-TATE was comparable to ^{64}Cu-CB-TE2A-Y3-TATE, one of the gold standard agents that has been investigated in other SSTR2-positive tumor models. Although ^{64}Cu-CB-TE2A-Y3-TATE was superior to ^{64}Cu-NODAGA-Y3-TATE in tumor to blood ratios at 4 hours, an advantage of NODAGA-Y3-TATE is that this agent allows for incorporation of both ^{64}Cu and ^{68}Ga, incorporates ^{64}Cu in high radiolabeling yields in a shorter period of time than ^{64}Cu-CB-TE2A-Y3-TATE, and provides a versatile PET probe for imaging SSTR2-positive tumors.

Acknowledgments

We extend our gratitude to Kathryn E. Day for her assistance in the biodistribution and imaging experiments.

Financial disclosure of authors: This research was supported by NIH/National Cancer Institute (NCI) 5R01CA064475 and a joint grant from the Office of Science (Biological and Environmental Research), U.S. Department of Energy, and the NIH (National Institute of Biochemical Imaging and Bioengineering) (DE-SC0008833). Small-animal imaging performed at Washington University is supported in part by NCI Cancer Center Support Grant P30 CA91842. UPCI-shared resources (In Vivo Imaging Facility) were used in this research, and this facility is supported in part by award NCI P30CA047904.

Financial disclosure of reviewers: None reported.

References

1. Papotti M, Kumar U, Volante M, et al. Immunohistochemical detection of somatostatin receptor types 1-5 in medullary carcinoma of the thyroid. Clin Endocrinol (Oxf) 2001;54:641–9, doi:10.1046/j.1365-2265.2001.01175.x.
2. Weiner RE, Thakur ML. Radiolabeled peptides in oncology: role in diagnosis and treatment. BioDrugs 2005;19:145–63, doi:10.2165/00063030-200519030-00002.
3. Kulaksiz H, Eissele R, Rossler D, et al. Identification of somatostatin receptor subtypes 1, 2a, 3, and 5 in neuroendocrine tumours with subtype specific antibodies. Gut 2002;50:52–60, doi:10.1136/gut.50.1.52.
4. Reubi JC, Waser B, Schaer JC, et al. Somatostatin receptor sst1-sst5 expression in normal and neoplastic human tissues using receptor autoradiography with subtype-selective ligands. Eur J Nucl Med 2001;28:836–46, doi:10.1007/s002590100541.
5. Janson ET, Stridsberg M, Gobl A, et al. Determination of somatostatin receptor subtype 2 in carcinoid tumors by immunohistochemical investigation with somatostatin receptor subtype 2 antibodies. Cancer Res 1998;58:2375–8.
6. Hofland LJ, Liu Q, Van Koetsveld PM, et al. Immunohistochemical detection of somatostatin receptor subtypes sst1 and sst2a in human somatostatin receptor positive tumors. J Clin Endocrinol Metab 1999;84:775–80, doi:10.1210/jcem.84.2.5497.
7. Schulz S, Schmitt J, Quednow C, et al. Immunohistochemical detection of somatostatin receptors in human ovarian tumors. Gynecol Oncol 2002;84:235–40, doi:10.1006/gyno.2001.6468.
8. Schulz S, Pauli SU, Handel M, et al. Immunohistochemical determination of five somatostatin receptors in meningioma reveals frequent overexpression of somatostatin receptor subtype sst2a. Clin Cancer Res 2000;6:1865–74.
9. Kikutsuji T, Harada M, Tashiro S, et al. Expression of somatostatin receptor subtypes and growth inhibition in human exocrine pancreatic cancers. J Hepatobiliary Pancreat Surg 2000;7:496–503, doi:10.1007/s005340070021.
10. Anderson CJ, Dehdashti F, Cutler PD, et al. 64Cu-TETA-octreotide as a PET imaging agent for patients with neuroendocrine tumors. J Nucl Med 2001;42:213–21.
11. Rogers BE, McLean SF, Kirkman RL, et al. In vivo localization of [(111)In]-DTPA-D-phe1-octreotide to human ovarian tumor xenografts induced to express the somatostatin receptor subtype 2 using an adenoviral vector. Clin Cancer Res 1999;5:383–93.
12. Wang ZZ, Qu W, Wang F, et al. Expression of somatostatin receptor reporter gene and its correlation with targeted imaging in vivo for detection of pancreas carcinoma. Zhonghua Zhong Liu Za Zhi 2005;27:663–6.
13. Baum EM, Knox HD, Miller TR, Watson AM. Nuclides and isotopes chart of the nuclides. Schenectady (NY): Knolls Atomic Power Lab; 2009.
14. Fani M, Andre JP, Maecke HR. Ga-68-PET: a powerful generator-based alternative to cyclotron-based PET radiopharmaceuticals. Contrast Media Mol Imaging 2008;3:53–63, doi:10.1002/cmmi.232.
15. Beattie BJ, Thorek DLJ, Schmidtlein CR, et al. Quantitative modeling of Cerenkov light production efficiency from medical radionuclides. PLoS One 2012;7:e31402, doi:10.1371/journal.pone.0031402.
16. Dothager RS, Goiffon RJ, Jackson E, et al. Cerenkov radiation energy transfer (CRET) imaging: a novel method for optical imaging of PET isotopes in biological systems. PLoS One 2010;5:e13300, doi:10.1371/journal.pone.0013300.
17. Delgado R, Sun YZ, Motekaitis RJ, et al. Stabilities of divalent and trivalent metal-ion complexes of macrocyclic triazatriacetic acids. Inorg Chem 1993;32:3320–6, doi:10.1021/ic00067a022.
18. Eisenwiener KP, Prata MI, Buschmann I, et al. NODAGATOC, a new chelator-coupled somatostatin analogue labeled with [67/68Ga] and [111In] for SPECT, PET, and targeted therapeutic applications of somatostatin receptor (hsst2) expressing tumors. Bioconjug Chem 2002;13:530–41, doi:10.1021/bc010074f.
19. Cooper MS, Ma MT, Sunassee K, et al. Comparison of (64)Cu-complexing bifunctional chelators for radioimmunoconjugation: labeling efficiency, specific activity, and in vitro/in vivo stability. Bioconjug Chem 2012;23:1029–39, doi:10.1021/bc300037w.
20. Lin M, Welch MJ, Lapi SE. Effects of chelator modifications on Ga-labeled [tyr]octreotide conjugates. Mol Imaging Biol 2013;15:606–13, doi:10.1007/s11307-013-0627-x.
21. Fani M, Del Pozzo L, Abiraj K, et al. PET of somatostatin receptor-positive tumors using 64Cu- and 68Ga-somatostatin antagonists:

the chelate makes the difference. J Nucl Med 2011;52:1110–8, doi:10.2967/jnumed.111.087999.
22. Alonso O, Gambini JP, Lago G, et al. In vivo visualization of somatostatin receptor expression with Ga-68-DOTA-TATE PET/CT in advanced metastatic prostate cancer. Clin Nucl Med 2011; 36:1063–4, doi:10.1097/RLU.0b013e31822920c9.
23. Klinaki I, Al-Nahhas A, Soneji N, et al. 68Ga DOTATATE PET/CT uptake in spinal lesions and MRI correlation on a patient with neuroendocrine tumor: potential pitfalls. Clin Nucl Med 2013;38: e449–53, doi:10.1097/RLU.0b013e31827a2325.
24. Naji M, Zhao C, Welsh SJ, et al. 68Ga-DOTA-TATE PET vs. 123I-MIBG in identifying malignant neural crest tumours. Mol Imaging Biol 2011;13:769–75, doi:10.1007/s11307-010-0396-8.
25. Thomas T, Zender S, Terkamp C, et al. Hypercortisolaemia due to ectopic adrenocorticotropic hormone secretion by a nasal paraganglioma: a case report and review of the literature. BMC Res Notes 2013;6:331, doi:10.1186/1756-0500-6-331.
26. Virgolini I, Ambrosini V, Bomanji JB, et al. Procedure guidelines for PET/CT tumour imaging with 68Ga-DOTA-conjugated peptides: 68Ga-DOTA-TOC, 68Ga-DOTA-NOC 68Ga-DOTA-TATE. Eur J Nucl Med Mol Imaging 2010;37:2004–10, doi:10.1007/s00259-010-1512-3.
27. Wadas TJ, Eiblmaier M, Zheleznyak A, et al. Preparation and biological evaluation of 64Cu-CB-TE2A-sst2-ANT, a somatostatin antagonist for PET imaging of somatostatin receptor-positive tumors. J Nucl Med 2008;49:1819–27, doi:10.2967/jnumed.108.054502.
28. Sprague JE, Peng Y, Sun X, et al. Preparation and biological evaluation of copper-64-labeled Tyr3-octreotate using a cross-bridged macrocyclic chelator. Clin Cancer Res 2004;10:8674–82, doi:10.1158/1078-0432.CCR-04-1084.
29. Nguyen K, Parry JJ, Rogers BE, et al. Evaluation of copper-64-labeled somatostatin agonists and antagonist in sstr2-transfected cell lines that are positive and negative for p53: implications for cancer therapy. Nucl Med Biol 2012;39:187–97, doi:10.1016/j.nucmedbio.2011.08.006.
30. Achilefu S, Wilhelm RR, Jimenez HN, et al. A new method for the synthesis of tri-tert-butyl diethylenetriaminepentaacetic acid and its derivatives. J Org Chem 2000;65:1562–5, doi:10.1021/jo991453t.
31. Anderson CJ, Jones LA, Bass LA, et al. Radiotherapy, toxicity and dosimetry of copper-64-TETA-octreotide in tumor-bearing rats. J Nucl Med 1998;39:1944–51.
32. Cheng Y, Prusoff WH. Relationship between the inhibition constant (K1) and the concentration of inhibitor which causes 50 per cent inhibition (IC50) of an enzymatic reaction. Biochem Pharmacol 1973;22:3099–108, doi:10.1016/0006-2952(73)90196-2.
33. Shokeen M, Zheleznyak A, Wilson JM, et al. Molecular imaging of very late antigen-4 (alpha4beta1 integrin) in the premetastatic niche. J Nucl Med 2012;53:779–86, doi:10.2967/jnumed.111.100073.
34. Qi J, Leahy RM. Resolution and noise properties of map reconstruction for fully 3-D PET. IEEE Trans Med Imaging 2000;19:493–506, doi:10.1109/42.870259.
35. Eric T. Clarke AEM. Stabilities of the Fe(III), Ga(III) and In(III) chelates of N,N,N′-triazacyclononanetriacetic acid. Inorg Chim Acta 1991;181:273–80, doi:10.1016/S0020-1693(00)86821-8.
36. Martell AE, Motekaitis RJ, Clarke ET, et al. Stability constants of metal complexes of macrocyclic ligands with pendant donor groups. Supramol Chem 1996;6:353–63, doi:10.1080/10610279608032555.
37. Bevilacqua A, Gelb RI, Hebard WB, et al. Equilibrium and thermodynamic study of the aqueous complexation of 1,4,7-triazacyclononane-N,N′,N′-triacetic acid with protons, alkaline-earth-metal cations, and copper(II). Inorg Chem 1987;26:2699–706, doi:10.1021/ic00263a029.
38. Velikyan I, Beyer GJ, Bergstrom-Pettermann E, et al. The importance of high specific radioactivity in the performance of 68Ga-labeled peptide. Nucl Med Biol 2008;35:529–36, doi:10.1016/j.nucmedbio.2008.03.002.
39. Velikyan I, Maecke H, Langstrom B. Convenient preparation of 68Ga-based PET-radiopharmaceuticals at room temperature. Bioconjug Chem 2008;19:569–73, doi:10.1021/bc700341x.
40. Edman P. On the mechanism of the phenyl isothiocyanate degradation of peptides. Acta Chem Scand 1956;10:761–8, doi:10.3891/acta.chem.scand.10-0761.
41. Edman P. Mechanism of the phenyl isothiocyanate degradation of peptides. Nature 1956;177:667–8, doi:10.1038/177667b0.
42. Banks PR, Paquette DM. Comparison of 3 common amine reactive fluorescent-probes used for conjugation to biomolecules by capillary zone electrophoresis. Bioconjug Chem 1995;6:447–58, doi:10.1021/bc00034a015.
43. Rogers BE, Manna DD, Safavy A. In vitro and in vivo evaluation of a 64Cu-labeled polyethylene glycol-bombesin conjugate. Cancer Biother Radiopharm 2004;19:25–34, doi:10.1089/108497804773391649.